Synergistic Antioxidant and Antimicrobial Efficacy of Novel Ag/Fe_3O_4 and S/Fe_3O_4 Nanohybrids Orchestrated by *Brassica napus* Phytochemicals

Hisham T. Hameed[1], *Sirhan. M.M[2]
[1,2]Department of Chemistry, College of Education for Pure Sciences, University of Anbar

*Corresponding author Email:muth_1974na@uoanbar.edu.iq

ABSTRACT

This study presents a simple green synthesis of **Fe_3O_4**-NPs and their nanohybrids (Ag/ **Fe_3O_4**and S/ **Fe_3O_4**) with the aid of *Brassica napus* leaf extract acting as a bioreducing and capping agent. The stabilization of the nanoparticles by the presence of plant phytoconstituents, especially phenolics, flavonoids and proteins, was determined using FTIR spectroscopy. The XRD analysis confirmed the presence of phase-pure magnetite NPs that crystalize in a cubic spinel structure with an average particle size of about 6.26 nm. TEM analysis showed quasi-spherical-shaped Fe_3O_4 NPs with an average particle size of ~7.5 nm with a narrow size distribution, whereas the FESEM studies showed particle sizes to be ~10.7 nm, which further increased to ~16.7 nm and ~19.18 nm for Ag/Fe_3O_4 and S/Fe_3O_4 , respectively, thus validating the successful synthesis of nanohybrids and modification of Fe_3O_4 NPs surfaces. Evaluation of the biological activity was carried out using antioxidant (DPPH) and antibacterial assays. Ag/Fe_3O_4 NPs displayed significant enhancement in antioxidant activity (88.32% scavenging ability, IC_{50} value = 199.10 µmol/L) compared to Fe_3O_4 (IC_{50} value = 422.12 µmol/L) and S/Fe_3O_4 NPs (IC_{50} value = 420.11 µmol/L), respectively, due to a synergistic effect. The antibacterial assay demonstrated that Ag/Fe_3O_4 NPs are more effective, with an inhibition zone of 18 mm and 19 mm with *E. coli* and *S. aureus*, respectively, as compared to other samples. The high surface reactivity, potential of electron transfer and synergistic effect of the physicochemical properties of the nanohybrids make them highly active. These results clearly show that green synthesized Ag/Fe_3O_4 nanohybrids are an excellent candidate for a variety of multifunctional platforms with sophisticated biomedical and antimicrobial uses.

Keywords: Green synthesis; Ag/Fe_3O_4 nanohybrids; *Brassica napus*; Antioxidant activity; Antibacterial activity.

Introduction

Green synthesis in nanochemistry has gained much attention owing to replacing toxic reducing agents and/or stabilizers with renewable biological resources. Green synthesis has not only reduced toxicity and confirmed biocompatibility, but it has also produced other significant products. In addition, the green synthesis of nanoparticles is consistent with the tenets of sustainable chemistry [1,2,3]. In plant-mediated methods of synthesis, the presence of bioactive compounds, such as phenols, flavonoids, sugars, amino acids, proteins, and other redox-active phytochemicals, can simultaneously reduce metal ions and cap newly formed nuclei. These compounds offer excellent stability and control levels of particle growth and aggregation that might occur within the system [4,5]. This is particularly important for nanosystems purportedly for biomedical applications, where substrate chemistry strongly influences colloidal equilibrium, cellular interactions, and organic

performance [6]. Recently, silver nanoparticles (Ag-NPs) have been very popular because they have a wide range of antimicrobial properties. Iron oxide nanoparticles (especially magnetite, Fe_3O_4, and related oxides) are also very useful because they can be recovered magnetically, are chemically stable, and can perform multifunctionality [7]. Ag-NPs' biomedical interest stems from their capacity to target two bactericidal mechanisms.

Recent studies indicate that green-synthesized silver nanoparticles (Ag-NPs) can disrupt bacterial membranes, alter permeability, generate reactive oxygen species (ROS), and infiltrate biofilms, offering crucial multi-targeted mechanisms to overcome conventional antibiotic resistance [8–12]. Plant-derived Ag-NPs also exhibit antioxidant and anticancer activities, driven by the bioactivities of the generated phytochemical corona [13]. For precise analytical characterization, techniques such as UV-Vis, FTIR, XRD, SEM, TEM, EDX, and DLS are commonly employed to ensure structural reproducibility and stability [14,15].

Similarly, plant-based iron oxide nanoparticles (Fe_3O_4mical traits including magnetism, low ductility, high surface area, and eco-friendliness—with potent bactericidal actions mediated via oxidative stress and biofilm inhibition, while facilitating magnetic recycling [16–17]. Recent literature confirms that these iron oxide nanomaterials possess plant-regulated antioxidant and anticancer properties [18]. Consequently, hybrid systems based on Fe_3O_4 are highly attractive; specifically, Ag-modified magnetite (Ag-Fe_3O_4) nanohybrids have shown enhanced antibacterial efficacy against pathogens such as *E. coli* and *S. coli* [19-20].

Building on these concepts, the current research utilizes *Brassica napus* leaf extract as a biological engine for synthesis. *Brassica* species are rich in bioactive phytochemicals, including polyphenols and glucosinolates, with recent evidence validating the strong antioxidant and antimicrobial potential of both *B. rapa* and *B. napus* matrices [28,29].

The abundance of phytochemicals in the *B. napus* leaf extract is why it is viable as a reducing agent and capping medium of the nanohybrid formation; furthermore, the biomolecules that are left on the surface of the oxide nanoparticle could be the reason why it is antibacterial and antioxidant, respectively [21]. The application of leaf extracts instead of synthetic reagents also offers costs in terms of sustainability, as leaf biomass is renewable and underutilized on a regular basis. To this end, *B. napus*-mediated synthesis, in addition to being the most convenient inexperienced chemistry option, is also a sensible biofunctionalization strategy [22]. Ag-Fe_3O_4 and S-Fe_3O_4 nanohybrids in this sense can be considered possible related design platforms. The Ag-Fe_3O_4 systems of silver and Fe_3O_4 of iron, respectively, confer strong antimicrobial and magnetic separability and structure-function conformation scaffolds [23,24]. Interfaces with sulfur-containing interfaces in sulfur-associated Fe_3O_4 hybrids allow coordination, dispersion and biomolecule interactions to be efficiently controlled (e.g., phytochemical stabilization). The functionality is enhanced by hydration, and the performance is enhanced by hydration, though the effects on biology will be dependent on size, crystallinity, oxidation state, surface charge, and capping chemistry. Sulfur nanoparticles: Antimicrobial activity based on the preparation methods [25]. Thus, the untested synthesis of Ag-Fe_3O_4 and S-Fe_3O_4 nanohybrids with the aid of *Brassica napus* leaf extract contributes to the sustainable and biodegradable design, and the biological activity of the green synthesized nanohybrids is assessed using antioxidant and antimicrobial tests.

MATERIAL AND METHODS

Collection of plant

Brassica napus leaves were amassed from the Abu Ghraib area of Baghdad, Iraq, in April and May 2025. The plant material is diagnosed and categorized via the Desert Studies Center at Anbar University. After elimination of contaminants, the leaves were dried in a shaded location at a consistent temperature until their weight stabilized, then ground into a fine powder. The prepared plant fabric was changed into stored in hermetic, opaque bins until delivery.

Chemicals

The experiment utilized (Fe $(NO_3)_2 \cdot 6H_2O$), and 25% (NaOH) from Fluka. Deionized water (DI) was used throughout the study. Utilization of ($AgNO_3$) at 98% analytical purity. Utilization of Sodium Sulfide (Na_2S_2) at 98% analytical purity. Chemicals were supplied by the Sigma-Aldrich company

Preparation of the crude Extract from Brassica napus

The plant extract was obtained out of Brassica napus leaves. These leaves are accrued, rinsed, dried and ground into a powder using an electric mixer. Sieving eliminated all the suspended solids. To a beaker containing 10 g of powder, add 200 mL of deionized water. The mixture was stirred with a magnetic stirrer. The mixture should be heated at 80°C for 30 min to obtain the brown extract, after which it should be cooled. Solution filtration followed. The plant extract was kept in a tumbler vial in the refrigerator until it was needed [26].

Green synthesis of iron oxide nanoparticles (Fe_3O_4)

This experiment was conducted with moderate changes, as described in some other place. Using a magnetic stir bar, dissolve 2.2 g of $Fe(NO_3)_2 \cdot 6H_2O$ in 200 mL of deionized water in a beaker. Then, upload the prepared 20 mL of plant extract carefully, Thereafter, the extract is added periodically, drop by drop, and the solution is continued to be stirred at 20°C. Then, increase the solution temperature to 80°C and adjust the pH by adding 1 M NaOH. This technique will lead to the formation of a brown precipitate, as demonstrated in the description given below. Let the precipitate cool to room temperature, then centrifuge at 1,200 rpm to remove any leftover fibre. Filter it through a Whatman No. 1 and wash 3 times in DI and absolute ethanol to remove impurities and dry in an oven at 60 °C for 2 hrs [27,28].

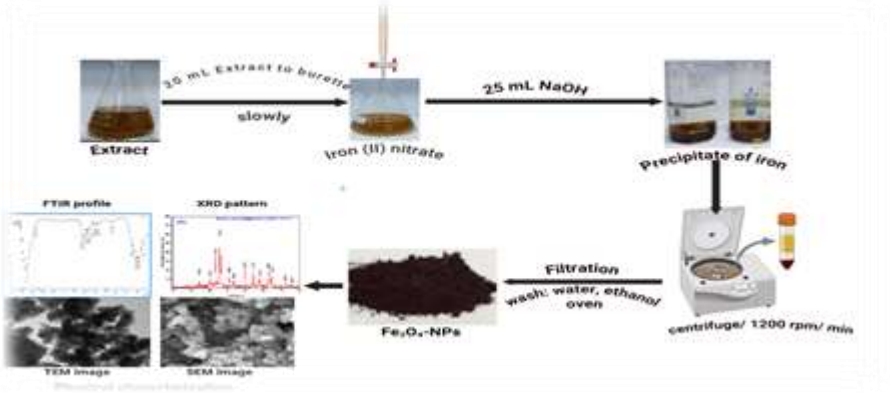


Figure 1: Schematic diagram of green synthesis and characterization of Fe_3O_4 (SPIONs)

Preparation of Ag/Fe_3O_4 and S/Fe_3O_4 Nanoparticles

The preparation of nanocomposites is carried out as defined by Okaieto *et al.* [29], who have outlined the use of the impregnation technique with moderate modifications with $AgNO_3$ or Na_2S_2 to obtain Ag and S nanoclusters, respectively. A 5-M ratio of $AgNO_3$ or Na_2S_2 with 1 g of Fe_3O_4 nanoparticles (green synthesis) was added to 50 mL of DI water. The aggregate was stirred in the dark at 80°C. The temperature should be maintained for 2 hr for complete synthesis. Thereafter, that, the colloidal aggregate is centrifuged at 1200 rpm for 15 min at 20°C, and the supernatant is collected for UV-vis evaluation. The pellet was dispersed in DI water and washed three times to remove impurities brought by Ag/NPs and S/NPs. Thereafter, the purified Ag/NPs and S/NPs were oven-dried at 60°C overnight, and the samples were ground with a mortar and pestle to harvest the powder.

CHARACTERIZATION

The main aim of such measurements was to know the shape, morphology and structure of the synthesized nanomaterials. The colour change of the reaction mixture was observed visually, as this change indicates that nanoparticles have formed. The identification of the functional groups present in Fe_3O_4 -NPs and nanocomposites in the 400–4000 cm^{-1} range was done using FTIR spectroscopy [36]. The X-ray diffraction (XRD; Panalytical X'Pert Pro) was used to investigate the crystalline structure of the as-synthesized samples using Cu-K alpha radiation (40 keV) and 15 mA, with scans being collected over a 2-theta range of 10-80°. The size and shape of the synthesized Fe_3O_4 -NPs were determined using transmission electron microscopy (TEM) that operated at 200 kV. Besides, field-emission scanning electron microscopy (FESEM; JEOL-JSM-7600F) was used in the study of the morphology and surface topography of the biosynthesized nanoparticles and nanocomposites. [30].

Study of the biological activities of Fe_3O_4, Ag/Fe_3O_4 and S/Fe_3O_4 (nanohybrids)

Two isolates of microorganisms were involved in this study, including Gram-positive *Staphylococcus aureus* and Gram-negative *Escherichia coli*. These microorganisms were used as test organisms to determine the inhibitory zone of Fe_3O_4 and nanocomposites, such as Ag/Fe_3O_4 and S/Fe_3O_4 (green synthesis). It would be interesting to understand the origin of the microorganisms to be used in determining the inhibitory zone of these specific isolates.

Antioxidant Activity OF Fe_3O_4 Ag/Fe_3O_4 and S/Fe_3O_4 samples.

The efficacy of nano-iron as an antioxidant was assessed using the DPPH (2,2-diphenyl-1-picrylhydrazyl) radical-scavenging assay to determine its ability to eliminate free radicals, as described in [38]. To obtain each concentration, 50 mg of the synthesized nano-iron sample was dissolved in 50 mL of ethanol, and the volume was then adjusted to 10 mL using ethanol to obtain final concentrations of 100, 200, 300, 400, and 500 µg/mL. A typical solution of ascorbic acid was prepared by dissolving 10 mg of ascorbic acid in 25 mL of distilled water, resulting in a final concentration of 10 mg/mL. Thereafter, the 60 µL of the standard ascorbic acid solution and the sample of iron nanoparticles were put in separate tubes. Each of the tubes was then incubated in darkness at room temperature (25°C), and 3 ml of DPPH solution was added to each tube and thoroughly mixed using a vortex mixer, and then the tubes were incubated in the dark for 30 minutes. Absorbance was determined at 517 nm, and the percentage of the DPPH radical inhibition was calculated using the following equation:

Inhibition percentage (% DPPH) = (A0 - A1 / A0 × 100)

where A0 is the absorbance of the control sample, and A1 is the absorbance of the reaction mixture.

Evaluation of the sensitivity of microbes to Fe_3O_4 Ag/Fe_3O_4 & S/Fe_3O_4 samples

To determine the effectiveness of the nanoparticle mixtures to stop the growth of bacteria, a test known as the well diffusion method was employed. The sample was prepared on a special plate, which is known as a Petri dish. The test helped determine whether the mixtures would be able to block the spread of some types of bacteria.

Preparation of nanohybrids wells by diffusion technique

Table 1 were used to prepare the concentrations of the nanocomposites, 5, 10, and 25 µg/mL, where each of the above concentrations were prepared as follows: It was autoclaved at 15 min and then 1 mL of the above solutions was added to a well and mixed using a mixer so that the material would be distributed evenly using the diffusion technique. The wells were dried by putting them in an incubator at 40 C during 24 hrs. (Antibiotic DA 10) -10 µg was the control sample. This test has been conducted in line with Kirby-Bauer. [31,32].

.

Muller-Hinton agar:

Mueller-Hinton agar is commonly believed to be the most effective medium that can be used to determine the sensitivity of bacteria to different drugs. The medium used in this investigation was Hi-Media, prepared according to the manufacturer's instructions. We combined 38 grams of Mueller-Hinton agar with 1 L of DI water to make the medium. Then the mixture was heated and stirred at certain intervals until all the powder was dissolved. We then autoclaved it for 15 min at 121°C and 1.5 psi. We then inoculated 20 mL of sterile medium in each Petri dish and allowed it to harden at room temperature. We incubated the dishes at 37°C for 24 hrs to ensure the environment was clean and to eliminate any excess moisture. When we were finished with the dishes, we put them in the fridge. For testing how sensitive bacteria are to different medications, this technique is crucial. These stages are also very important to follow precisely in order to obtain the appropriate findings.[33]

Table 1: Bacterial Types Used to Determine the Zone of Inhibition

No.	Bacterial isolates	Gram dye	Source
1	*Escherichia coli*	G^-	*Al-Ramadi Educational*
2	*Staphylococcus aureus*	G^+	*Hospital*

Spread of wells

The nanohybrids were carefully placed in the wells. There was at least 24 mm of space between each well. This procedure was done to ensure that the inhibition areas did not interfere with each other's ways. The dishes were inverted and maintained at a temperature of 37°C for a duration of 24 hrs.

Measurement of the inhibition zone:

Using a millimeter ruler, we measure the diameter of each well cautiously. The measured area includes the entire clear area surrounding the antibiotic well and the well itself. The clear area shows how well the antibiotic is stopping bacteria from growing as it spreads.

RESULT AND DISCUSSION

The (FTIR) spectra of magnetite (Fe_3O_4) nanoparticles and their nanohybrids (Ag/Fe_3O_4 and S/Fe_3O_4). A wide absorption band between 3475 and 3415 cm^{-1} is due to O–H stretching vibrations. This shows that phenolic compounds and flavonoids are present and are acting as reducing and

stabilizing agents. This is in line with recent progress in the synthesis of nanoparticles using plants [34]. The peaks at 16351616 cm^{-1} are either because of the stretching of C=O bonds in amides or vibration of C=C bonds in aromatic rings. This implies that the proteins and polyphenols are sticking to the surface of the nanoparticles, forming a stable layer that covers the nanoparticles. When these molecules stick to the surface of the nanoparticle, they seem to form this layer, which is called a bio-capping layer [35]. The band at a position of 1558 cm^{-1} is designated to the N-H bending (amide II), thus showing that nitrogen-based biomolecules are used to stabilize nanoparticles. The peaks between 1382 and 1338 cm^{-1} are due to C-N stretching or O-H bending, and the peaks between 1109 and 1067 cm^{-1} are because of C-O stretching vibrations. This implies that alcohol and polysaccharides exist and assist in maintaining the stability of the colloids. Extra bands in the 999--850 cm -1 range indicate that the structure has altered due to the addition of silver and its reaction with the Fe_3O_4 matrix. This is in line with recent research on metal–magnetite nanocomposites [36]. The strong absorption bands seen in the low wavenumber range (628–470 cm^{-1}) are which show that crystalline magnetite has formed. Notably, slight changes in the positions and intensities of the peaks in the nanohybrids compared to pure Fe_3O_4 show that surface functionalization and interfacial interactions have worked, especially in the S/Fe_3O_4 system. This study follows the recent reports, which put a lot of emphasis on the role of surface engineering in enhancing the performance of nanoparticles. These results prove the efficiency of green synthesis using Brassica napus to produce stable and functional nanostructures with promising applications in nanotechnology.

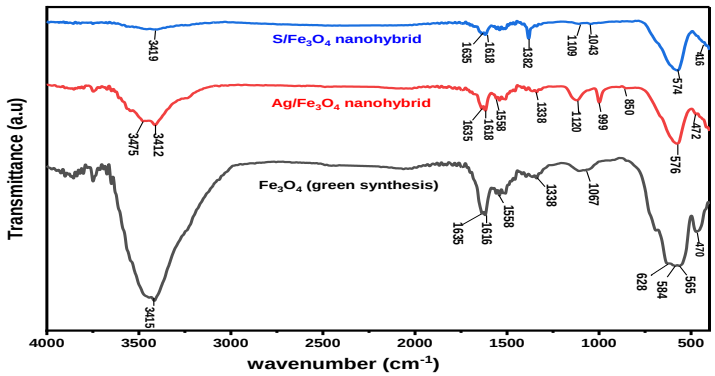


Figure 2: FTIR spectrum of Fe_3O_4 (SPIONs) synthesized from *Brassica napus* (green synthesis), Ag/Fe_3O_4, and S/Fe_3O_4 nanohybrids

Transmission electron microscopy (TEM) analysis The TEM picture and the histogram of the size distribution of the particles that

have been synthesized indicate that the green synthesized Fe_3O_4 -NPs are quasi-spherical in shape and are tightly clustered together. This aggregation can be mostly explained by the high surface energy and the strong magnetic dipole-dipole interactions of magnetite nanoparticles. Phytochemicals, including polyphenols, flavonoids and proteins, are reducing and capping agents in green synthesis systems, and their stabilization effect is generally weaker than that of synthetic surfactants, which is one of the factors that has contributed to the partial aggregation of the micrograph [37]. Although the observed agglomeration was noted, the primary particles remained uniform and nanoscale, confirming that the green synthesis method provided good control over nucleation and growth. The corresponding histogram shows that the mean size of the particles is approximately 7.5 nm, and the standard deviation of the sizes is also 1.09 nm, which means the size distribution is rather narrow. The red Gaussian fitting curve indicates that the particle sizes are distributed in a near-normal way, which is understandable in terms of the high reproducibility and well-controlled synthesis conditions. This level of uniformity is generally linked to optimized parameters of synthesis (pH, temperature, and extract concentration) that affect the reduction kinetics and particle stabilization [38].

The small particle size (<10 nm) suggests that the Fe_3O_4 nanoparticles are probablysuperparamagnetic, which is a property desirable in biomedical applications such as targeted drug delivery, magnetic resonance imaging (MRI), and hyperthermia therapy. The noted structural features, small size, quasi-spherical geometry and acceptable dispersion are compatible with earlier reported green-synthesized magnetite nanoparticles and confirm the appropriateness of this technique in the production of functional nanomaterials [39]. Overall, the combination of TEM and particle size analysis proves the successful synthesis of the Fe_3O_4 nanoparticles using a green approach, which resulted in the relatively homogeneous, ultrasmall nanoparticles with minor aggregation, which is inherent to magnetic nanomaterials

.

Field emission scanning electron microscopy (FESEM) analysis

The particle size of the green-synthesized Fe_3O_4 -NPs using *Brassica napus* extract (mean ≈ 10.7 nm, SD ≈ ±2.8 nm) gives a useful point of reference in understanding the structural changes that occur following the hybridization of Ag and S. The mean size is relatively small, and the standard deviation is moderate, which means that the green synthesis route encouraged the efficient nucleation and controlled growth, but the observed dispersion suggests the inherent variability of phytochemical-mediated reduction. Bioactive compounds include phenolics, flavonoids and proteins found in plant extracts such as *Brassica napus* and may act as reducing agents and capping agents but with weaker stabilization properties than synthetic surfactants, so some partial aggregation and moderate polydispersity should be expected [39].

When the size of Fe_3O_4 -NPs is compared with the size of the nanohybrid results, it is clear that there was a systematic increase in the size of the particle, reaching 16.7 nm (SD 4.3 nm) in the case of the Ag/Fe_3O_4 and 19.18 nm (SD 4.46 nm) in the case of the S/Fe_3O_4 . This tendency facilitates effective surface alteration and hybrid formation, as the addition of secondary components is bound to shift the behaviour of nucleation and growth as well. The Ag nanoparticles deposited on the surface of Fe_3O_4 in Ag/Fe_3O_4 form decorated or core/shell-like morphologies. The Ag^+ ions present in the synthesis may have added more nucleation sites and forced heterogeneous growth, leading to particle enlargement and a wider size distribution [48]. Moreover, silver

atoms may reduce the energy differences on the surfaces and encourage the partial coalescence of neighboring particles. In the case of the S/Fe_3O_4 nanohybrid, the rise in the average size to approximately 19.18 nm, with a slightly higher standard deviation, suggests a greater impact of the addition of sulfur in the particle assembly. Sulfur species can extensively interact with iron oxide surfaces through FeS bonding and adsorption, and thus promote interparticle bridging and cluster formation and also generate larger apparent particle sizes in SEM micrographs [40]. Additionally, the sulfur modification can change the charge of the surface and decrease the electrostatic repulsion, which will lead to increased aggregation resulting in less uniform growth compared to the Ag-modified system. By comparing these results to the previously discussed SEM images, it is clear that there is a morphological progression from $Fe_3O_4 \rightarrow Ag/Fe_3O_4 \rightarrow S/Fe_3O_4$: [41] (i) Initially small nanoparticles with moderate aggregation (10.7 nm), (ii) increased size and improved surface decoration in Ag/Fe_3O_4 (16.7 nm), and (iii) [51] more pronounced aggregation and larger clusters in S/Fe_3O_4 (19.18 nm). The underlying causes of this development include the surface chemistry modification, secondary phase deposition, and interparticle interactions. Notably, even with this size increase, all systems are at the nanoscale (<20 nm), which is favorable to superparamagnetic behaviour and high surface area the latter of which are favorable to catalysis, antimicrobial activity, and biomedical applications. The observed size evolution and morphology are consistent with previous work on green-synthesized iron oxide nanohybrids, where hybridization generally leads to an increase in particle size and a change in aggregation due to altered surface energetics and reaction pathways [42].

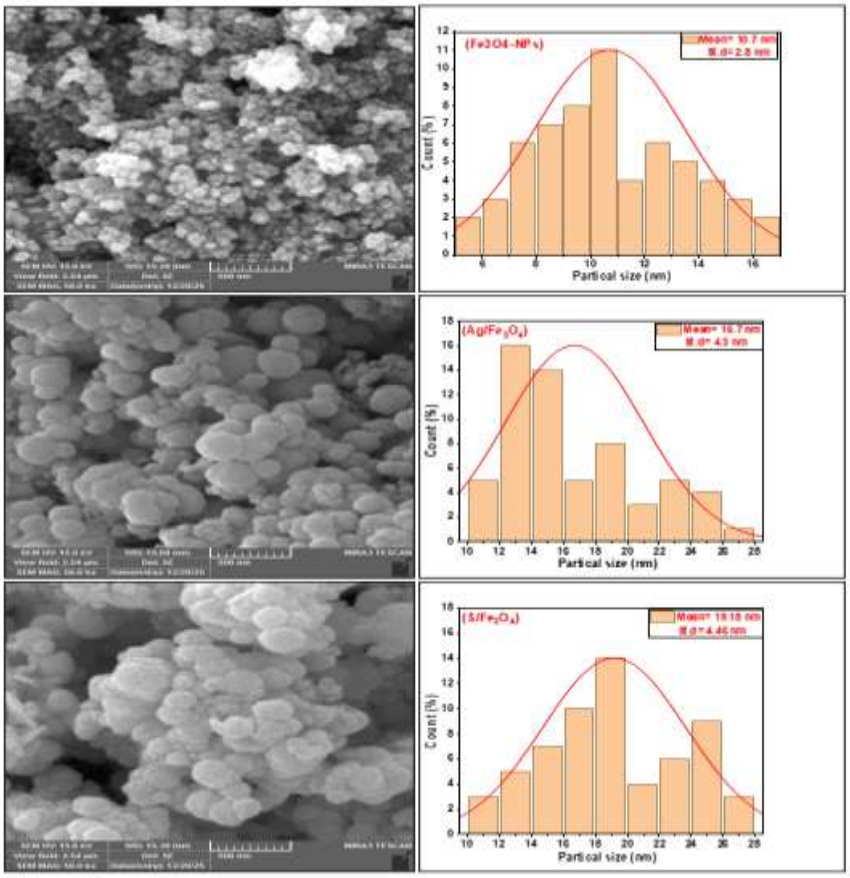


Figure 3: **Field emission scanning electron microscopy (FESEM) analysis**

X-ray diffraction (XRD) analysis

In figure 4 the (XRD) pattern of the green-synthesized Fe_3O_4 nanoparticles clearly shows a set of well-defined diffraction peaks at approximately 2θ 30, 35, 43, 57, and 62 degrees, which can be indexed to the crystallographic planes (220), (311), (400), (511), and (440), respectively. This is in excellent agreement with the standard magnetite phase (JCPDS card No. 19-0629), which confirms the successful synthesis of Fe_3O_4 with a cubic inverse spinel structure. High phase purity and crystallinity have been widely reported with green-synthesized Fe_3O_4 nanoparticles with similar positions of the peak and indexing [53,54]. The strongest peak of diffraction found at the (311) plane indicates a favourable orientation and strong crystallographic order in the nanoparticles. The lack of other peaks associated with other secondary phases, such as hematite (Fe_2O_3) or maghemite (γ-Fe_2O_3), is yet another confirmation that the material synthesized is phase-pure magnetite, commonly obtained in controlled systems of green synthesis due to the stabilizing effect of plant phytochemicals [56]. Further, the apparent expansion of the diffraction peaks is a sign of the nanoscale size of the particles. The Debye Scherrer equation was used to determine the crystallite size.

$$D = \frac{0.9\,\lambda}{\beta cos\theta}$$

The determined crystal sizes of the crystallites lie between 4.6 and 7.3 nm with an average size of 6.26 nm. This is small in relation to green-synthesized Fe_3O_4 nanoparticles, which are dependent on the synthesis conditions [55]. Comparing these XRD results with TEM and SEM results, a definite and scientifically coherent trend can be observed. The XRD crystal size (~6 nm) is smaller than the crystal size measured by TEM (~10.7 nm) and SEM (~16-19 nm). This difference is predicted and can be attributed to the inherent differences between the methods. XRD determines the size of the coherent crystalline domains, whereas TEM determines the actual particle size, which can be several crystallites. SEM, in contrast, can be the manifestation of larger agglomerated structures because of the clustering of the particles. Additionally, the observed increase in particle size between the TEM and SEM analyses can be attributed to the organic capping agents present in the plant extract used for green synthesis [44].

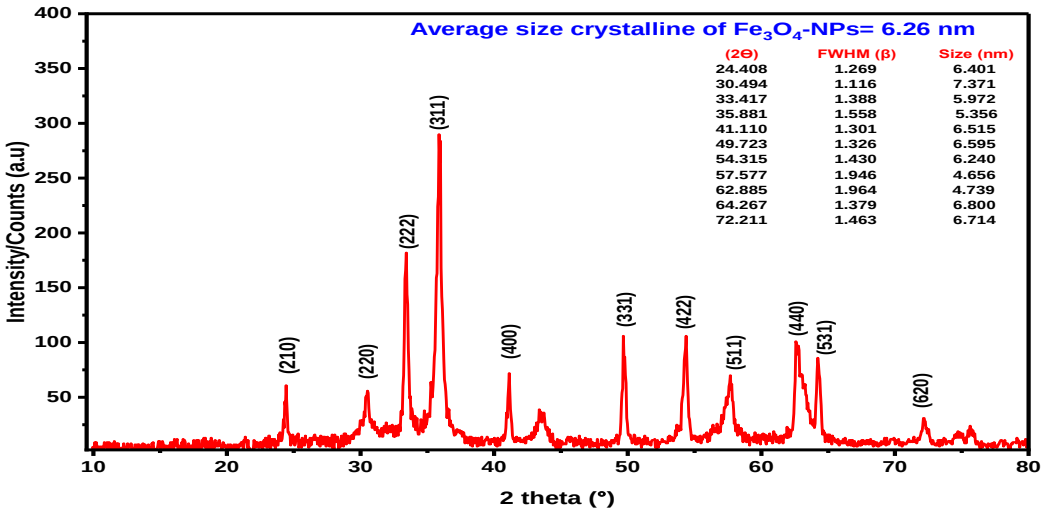


Figure 4: shows the XRD pattern of Fe_3O_4 nanoparticles (green synthesis). It has unique diffraction peaks that correspond to different crystallographic planes. This confirms that a spinel cubic structure has formed. **(JCPDS card 19-0629**)

In vitro biological studies

Antioxidant efficacy testing (DPPH test)

Nanotechnology, based on transition metals, namely magnetite (Fe_3O_4), is an essential area in developing modern antioxidants. This analysis aims to interpret the findings of the DPPH free radical scavenging assay of three compounds : pure iron oxide (Fe_3O_4), silver-doped iron oxide (Ag/Fe_3O_4) and sulfur-modified iron oxide (S/Fe_3O_4). Based on the IC_{50} and redox activity ratio, the DPPH assay aims to measure the compounds' ability to inhibit stable DPPH free radicals, thus highlighting their potential as bio-antioxidants. The best one is the Ag/Fe_3O_4 compound, which has the highest scavenging efficiency (88.32%) and the lowest IC_{50} (199.10 µmol /L), which means it is better. This phenomenon occurs because combining Fe_3O_4 with the silver nanoparticles creates a synergistic effect that enhances their superiority. The silver nanoparticles amplify the reactive surface area and enhance the compound's ability to donate electrons to DPPH free radicals and thus increase its antioxidant activity. This finding corresponds with other studies that have been conducted recently with silver being used as an antioxidant enhancer. Although the S/Fe_3O_4 compound shows a good activity, slightly higher than that of pure Fe_3O_4, the sulfur modification is thought to either add functional groups (S groups) or provide good surface coverage to the formation of particles or the enhancement of activity.

The sulfur groups are rather inactive in terms of antioxidant activity or transition metal filtering, which contributes to a slight augmentation of antioxidant action in comparison to pure iron nanoparticles. While Fe_3O_4 shows reasonable activity (IC_{50} = 422.12 µmol/L), closely related to the sulfur compound, the activity of the magnetic iron oxide nanoparticles can be explained by their ability to react with free radicals through surface redox reactions or by surface radical stabilization. Statistical and theoretical variations show that the silver addition was not a mere addition but a synergistic alteration that seemingly boosted the activity of the compound by a very significant margin. This ability is credited to the fact that silver nanoparticles (Ag/NPs) catalyze and facilitate the transfer of electrons to the stable DPPH radical. The presence of magnetite (Fe_3O_4) gives it structural support and increases the reactive surface area, leading to an oxidation capacity that greatly exceeds the product of the efficiencies of the two elements, individually. The approximate values of IC_{50} of the sulfur (420.10) and pure iron (422.12) mixtures show that the sulfur modification produced only a slight increase in the stability instead of a radical improvement of the quenching mechanism. The length of the sulfur compound is probably limited by depleting agglomeration and maintaining an optimal distribution of nanoparticles, and therefore, the anti-ageing properties of the Fe_3O_4 surface are more likely to be retained over a longer period. The oxidation rate (88.32%), which is the rate at which an oxidant combats the antioxidants, was found to be very high in the iron and silver nanoparticle composite (88.32%), which was many times higher than the reference standard (ascorbic acid), a reference standard used to measure the antioxidant strength of a substance. This outcome will categorize the composite as a material with greater antioxidant activity, and thus, it is highly promising for future therapeutic applications. All the composites exhibited a progressive reduction in the ability to scavenge free radicals with a decrease in concentration, which is one of the important

characteristics to verify the validity of test results. The outcomes of the oxidative strength-based analysis show a successful model of nanoparticle surface engineering, generated by introducing silver nanoparticles into Fe_3O_4 particles, aimed at improving biological performance. The low IC_{50} value of the Ag/Fe_3O_4 composite is a promising platform where the magnetic strength (of Fe_3O_4), which is useful in therapeutic targeting, combines with the high antioxidant strength (of silver), which makes it an ideal candidate to be used in biotechnology applications (such as oxidative stress treatment or drug delivery).

Table 2: Comparison of the effectiveness of modified nano-free radical scavenging at different concentrations, and the value of IC_{50}.

Scavenging (%)			Concentration ($\mu L\ ml^{-1}$)
Fe_3O_4-NPs	Ag /Fe_3O_4-nanohybrid	S/Fe_3O_4-nanohybrid	
$77.65^{a} \pm 0.2$	$88.32^{a} \pm 0.23$	$81.03^{a} \pm 0.22$	500
$76.01^{b} \pm 0.4$	$81.01^{b} \pm 0.24$	$76.02^{b} \pm 0.33$	400
$72.34^{c} \pm 0.54$	$73.12^{c} \pm 0.11$	$70.44^{c} \pm 0.12$	300
$58.53^{cd} \pm 1.44$	$54.13^{cd} \pm 2.98$	$59.85^{cd} \pm 2.56$	200
$51.542^{d} \pm 0.30$	$51.53^{d} \pm 0.38$	$51.542^{d} \pm 0.38$	100
422.12	199.10	420.11	IC_{50}
	77.07^{dc}		Ascorbic ($10mg.ml^{-1}$)
1.432		2.54	$LSD_{0.05}$

The functional specificity of iron oxide nanoparticles (Fe_3O_4) is due to their high capability of scavenging free radicals (like DPPH). Research has shown that the concentration and efficiency of inhibition have a direct relationship, with a range of 29% to 74% [45.46]. The adoption of "green manufacturing" techniques has further enhanced the reduction capacity of these particles (SPIONs) to over 80%, an efficiency approaching that of ascorbic acid. These findings are consistent with the study by Al-Ani and Altameme (2023) on Ag-Fe hybrid systems, where the combination of silver and iron creates a synergistic effect that enhances chemical stability and provides additional active sites for electron exchange.[59] These particles, in a mechanistic way, act as nanozymes, which mimic the activity of catalase and peroxidase enzymes. This helps in the breakdown of hydrogen peroxide and prevents cellular components from undergoing programmed oxidative stress [47,48]. It has also been shown that these particles are highly efficient as green nanocatalysts in the synthesis of highly potent oxazole derivatives, which are used as antioxidants in comparison with the standard compounds. Modification of surfaces is a key factor in promoting performance; organic coatings or reactive groups (including phenols) promote the donation of protons or electrons to neutralize free radicals [49]. A special synergy is also found between mineral core

and a biosphere rich in phytochemicals in biosystems prepared using plant extracts

Ag-Fe hybrid systems provide a high-quality model of the biological activity; the silver coating, rich in flavonoids, increases the concentration of O-H groups that can interact [63,64]. The research establishes the superiority of these hybrid systems as systems which concentrate and amplify the activity of antioxidant bonds. In the context of environmental applications, the study by Yildiz (2024) demonstrated that these particles, at a concentration of 1.5%, completely inhibit the growth of brown rot, highlighting their potential as wood preservatives. These nanoenzymes are strategically important because they are highly stable, reusable, and can be targeted to a specific point using magnetism [65]. Nevertheless, there is still a need to carry out intensive scientific research on the issues of biosafety and tissue distribution to ensure the safe implementation of these technologies in the laboratory, clinical, and industrial applications [66].

Inhibition of Some Bacterial Isolates by Fe_3O_4 -NPs and nanohybrids

Table 3 presents the results of a comparative study on the effectiveness of three nanoparticles (pure iron, iron-silver, and iron-sulfur) in inhibiting the growth of two bacterial strains, *Escherichia coli* and *Staphylococcus aureus*. The iron-silver nanoparticle had the highest values of inhibition zones as compared to the other prepared nanoparticles, reaching 18 ± 1.2 mm against *E. coli* and 19 ± 1.0 mm against *S. aureus*. This result is due to the synergistic effect of silver with iron nanoparticles, which have been shown to have synergistic effects in bactericidal processes that include the release of ions that interact with DNA and disrupt cellular metabolism proteins [67]**.** They also cause oxidative stress in the bacterial cell, destruction of the cell membrane, and programmed cell death. [68]**.**

[50].

Table 3: The effect of different treatments of nano-iron and combined elements on some bacterial isolates, inhibition diameters are measured in mm.

Treatment	Concentrations µg.ml^{-1}	*Staphylococcus aureus* G^+	*Escherichia coli* G^-
Fe_30_4-NPs	5	13±1.4	11±1.9
	10	16±1.0	14±1.7
	25	16±0.1	15±0.4
Ag/ Fe_3O_4	5	17±1.4	14±1.0
	10	17±1.0	16±1.5
	25	18±1.2	19±1.0
S/Fe_3O_4	5	9±1.0	9±0.0
	10	12±1.0	11±1.0
	25	13±1.0	15±1.0

Antibiotic (DA 10) + control	15±1	13±1
P value Between tested groups and control	0.0001	0.05
LSD 5%	0.082	0.073

The statistical analysis and research findings demonstrated that bimetallic (Ag-Fe) nanoparticles, which were prepared using the techniques of "green manufacturing", are superior in their inhibitory effects on bacterial isolates in comparison with monometallic systems and traditional antibiotics (DA10). The research discovered that the attaching ability of sulfur can diminish the inhibitory activity of Gram-positive bacteria because of the covering of active functional groups. There was also data to confirm the principle of dose-dependent response in antimicrobial activity with respect to strain susceptibility. *S. aureus* (Gram-positive) was found to be more susceptible than *E. coli* (Gram-negative).

This phenomenon is due to the structural differences seen in the cell wall, where the lack of a complex outer membrane in Gram-positive bacteria facilitates the penetration and interaction of the nanoparticles with the thick peptidoglycan layer. The paper shows that the polyphenol-rich plant extracts can be used as reducing and coating agents, thereby providing the particles with chemical stability and inhibiting aggregation, which in turn increases the effective surface area of the particles. High capacity to scavenge free radicals (DPPH) and induce the formation of reactive oxygen species (ROS), which cause oxidative stress, resulting in cell membrane rupture and damage to the DNA of pathogens and cancer cells, demonstrates the biological mechanism of action of these compounds.

The research finds that silver nanoparticle modification is an ideal approach towards the development of promising agents to combat microbial infections and tumours as the rate of antibiotic resistance is ever-increasing.



Figure 5: Inhibition zones of 25 µg.ml^{-1} (**Ag/Fe_3O_4**) nanohybrid right for *S. aureus* and left for *E. coli*.

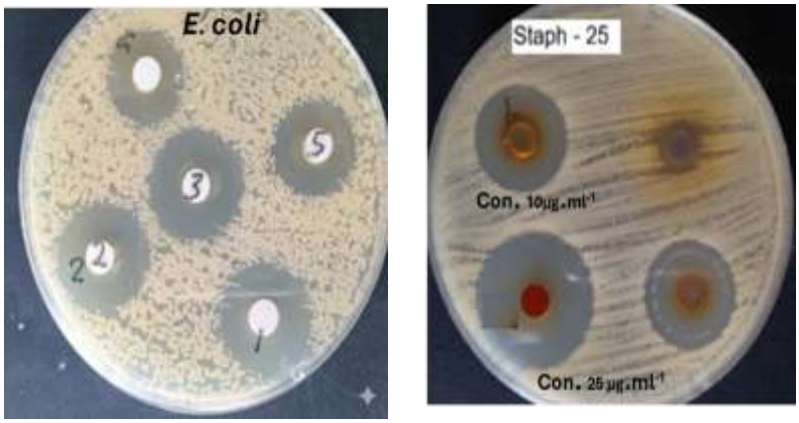


Figure 6: Antibacterial activity and inhibition zones of bimetallic (**Ag/Fe_3O_4**) nanohybrid at a concentration of 25 µg/ml against *S. aureus* and *E. coli*.

CONCLUSION

This study has successfully developed an environmentally friendly green synthesis route to the preparation of Fe_3O_4 nanoparticles and their Ag- and S-based nanohybrids using *Brassica napus* leaf extract. The dual role of the phytochemical constituents of the extract as reducing and stabilizing agents played a key role in the formation of well-defined, nanoscale structures. Successful surface modification was demonstrated by structural characterization (the successful formation of phase-pure magnetite with high crystallinity) and morphological analyses (systematic increase in particle size upon hybridization, i.e., between ~10.7 nm with Fe_3O_4 and ~16.7 nm with Ag/Fe_3O_4 and S/Fe_3O_4 , respectively). Biological studies showed that adding silver greatly improved both the antioxidant and antibacterial properties. The highest free radical scavenging activity and the lowest IC_{50} value were found in the Ag/Fe_3O_4 nanohybrid, which had the best antibacterial activity against the Gram-positive and Gram-negative bacteria. Such an increased activity is also explained by the synergistic effect of the magnetic core of Fe_3O_4 and the bioactive silver constituent, which enhances surface reactivity and electron transfer processes. In general, the results indicate that green-synthesized Ag/Fe_3O_4 nanohybrids are a promising multifunctional tool to be used in advanced biomedical applications. Future research ought to address the toxicity, in *vivo* testing, and scaled studies to help them become practical medical and environmental applications.

LIMITATIONS

Although it is a useful study to provide information about the antibacterial properties of *Brassica napus* Fe_3O_4 -NPs and nanohybrids, it is limited to in vitro studies. Further studies are needed to confirm their efficiency under working conditions and to understand the possible harmful effects of these nanocomposites. Furthermore, the study did not cover the whole spectrum of microbial strains. Further research may extend the study to a broader range of pathogens to fully evaluate the antimicrobial efficacy of the nanocomposites.

RECOMMENDATIONS

The results suggest that additional controlled experiments, especially on living organisms, are needed to assess the efficiency of the synthesized *Brassica napus* Fe_3O_4 NPs and nanohybrids as potential antibacterial agents. Further studies could be done to use these nanocomposites in real time, like in mouthwash to fight *Escherichia* and *streptococcal* bacteria. Moreover, further investigation is recommended for the durability, longevity, and real-world uses of the nanocomposites.

DECLARATIONS

Ethical Approval: Ramadi Teaching Hospital approved the research according to the ethical standards of research on human subjects.
Escherichia bacteria were isolated from the sputum of patients at Ramadi Teaching Hospital for Maternity and the Consultative Clinic for Chest Diseases. This sample was then taken to the laboratory and transplanted onto the already prepared implants, and the rest of the bacteria were taken from the soil.

AUTHOR CONTRIBUTIONS

Hisham experimented and carried out the DFT calculation. Dr Muthana Mohammed Sirhan wrote and revised the manuscript. Each of the authors was satisfied with the final version of this manuscript.

REFERENCES

[1] M. A. Huq, M. Ashrafudoulla, M. M. Rahman, S. R. Balusamy, and S. Akter, "Green Synthesis and Potential Antibacterial Applications of Bioactive Silver Nanoparticles: A Review," *Polymers (Basel).*, vol. 14, no. 4, pp. 1–22, 2022, doi: 10.3390/polym14040742.

[2] C. Vanlalveni, S. Lallianrawna, A. Biswas, M. Selvaraj, B. Changmai, and S. L. Rokhum, "Green synthesis of silver nanoparticles using plant extracts and their antimicrobial activities: a review of recent literature," *RSC Adv.*, vol. 11, no. 5, pp. 2804–2837, 2021, doi: 10.1039/d0ra09941d.

[3] S. Shahzadi, S. Fatima, Q. Ul Ain, Z. Shafiq, and M. R. S. A. Janjua, "A review on green synthesis of silver nanoparticles (SNPs) using plant extracts: A multifaceted approach in photocatalysis, environmental remediation, and biomedicine," *RSC Adv.*, vol. 15, no. 5, pp. 3858–3903, 2025, doi: 10.1039/d4ra07519f.

[4] H. Bahrulolum *et al.*, "Green synthesis of metal nanoparticles using microorganisms and their application in the agrifood sector," *J. Nanobiotechnology*, vol. 19, no. 1, pp. 1–26, 2021, doi: 10.1186/s12951-021-00834-3.

[5] K. Okaiyeto, H. Hoppe, and A. I. Okoh, "Plant-Based Synthesis of Silver Nanoparticles Using Aqueous Leaf Extract of Salvia officinalis: Characterization and its Antiplasmodial Activity," *J. Clust. Sci.*, vol. 32, no. 1, pp. 101–109, 2021, doi: 10.1007/s10876-020-01766-y.

[6] J. Schubert and M. Chanana, "Coating Matters: Review on Colloidal Stability of Nanoparticles with Biocompatible Coatings in Biological Media, Living Cells and Organisms," *Curr. Med. Chem.*, vol. 25, no. 35, pp. 4553–4586, 2018, doi: 10.2174/0929867325666180601101 8

59.

[7] E. Urnukhsaikhan, B. E. Bold, A. Gunbileg, N. Sukhbaatar, and T. Mishig-Ochir, "Antibacterial activity and characteristics of silver nanoparticles biosynthesized from Carduus crispus," *Sci. Rep.*, vol. 11, no. 1, pp. 1–12, 2021, doi: 10.1038/s41598-021-00520-2.

[8] T. R. Anju *et al.*, "Green synthesis of silver nanoparticles from Aloe vera leaf extract and its antimicrobial activity," *Mater. Today Proc.*, vol. 43, pp. 3956–3960, 2020, doi: 10.1016/j.matpr.2021.02.665.

[9] M. Oves *et al.*, "Green synthesis of silver nanoparticles by Conocarpus Lancifolius plant extract and their antimicrobial and anticancer activities," *Saudi J. Biol. Sci.*, vol. 29, no. 1, pp. 460–471, 2022, doi: 10.1016/j.sjbs.2021.09.007.

[10] Y. Khane *et al.*, "Green Synthesis of Silver Nanoparticles Using Aqueous Citrus limon Zest Extract: Characterization and Evaluation of Their Antioxidant and Antimicrobial Properties," *Nanomaterials*, vol. 12, no. 12, 2022, doi: 10.3390/nano12122013.

[11] M. Khatun, Z. Khatun, M. R. Karim, M. R. Habib, M. H. Rahman, and M. A. Aziz, "Green synthesis of silver nanoparticles using extracts of Mikania cordata leaves and evaluation of their antioxidant, antimicrobial and cytotoxic properties," *Food Chem. Adv.*, vol. 3, no. May, p. 100386, 2023, doi: 10.1016/j.focha.2023.100386.

[12] M. Ansari *et al.*, "Plant mediated fabrication of silver nanoparticles, process optimization, and impact on tomato plant," *Sci. Rep.*, vol. 13, no. 1, pp. 1–19, 2023, doi: 10.1038/s41598-023-45038-x.

[13] T. Ongtanasup, P. Kamdenlek, C. Manaspon, and K. Eawsakul, "Green-synthesized silver nanoparticles from Zingiber officinale extract: antioxidant potential, biocompatibility, anti-LOX properties, and in silico analysis," *BMC Complement. Med. Ther.*, vol. 24, no. 1, pp. 1–20, 2024, doi: 10.1186/s12906-024-04381-w.

[14] A. Wasilewska, U. Klekotka, M. Zambrzycka, G. Zambrowski, I. Święcicka, and B. Kalska-Szostko, "Physico-chemical properties and antimicrobial activity of silver nanoparticles fabricated by green synthesis," *Food Chem.*, vol. 400, no. January 2022, 2023, doi: 10.1016/j.foodchem.2022.133960.

[15] O. Elkhateeb, M. B. Atta, and E. Mahmoud, "Biosynthesis of iron oxide nanoparticles using plant extracts and evaluation of their antibacterial activity," *AMB Express*, vol. 14, no. 1, 2024, doi: 10.1186/s13568-024-01746-9.

[16] V. Archana, J. Joseph Prince, and S. Kalainathan, "Simple One-Step Leaf Extract-Assisted Preparation of α - Fe2O3Nanoparticles, Physicochemical Properties, and Its Sunlight-Driven Photocatalytic Activity on Methylene Blue Dye Degradation," *J. Nanomater.*, vol. 2021, 2021, doi: 10.1155/2021/8570351.

[17] D. A. Demirezen, Ş. Yılmaz, D. D. Yılmaz, and Y. Ş. Yıldız, "Green synthesis of iron oxide nanoparticles using Ceratonia siliqua L. aqueous extract: improvement of colloidal stability by optimizing synthesis parameters, and evaluation of antibacterial activity against Gram-positive and Gram-negative bacteria," *Int. J. Mater. Res.*, vol. 113, no. 10, pp. 849–861, 2022, doi: 10.1515/ijmr-2022-0037.

[18] H. Al-Karagoly *et al.*, "Green synthesis, characterization,

cytotoxicity, and antimicrobial activity of iron oxide nanoparticles using Nigella sativa seed extract," *Green Process. Synth.*, vol. 11, no. 1, pp. 254–265, 2022, doi: 10.1515/gps-2022-0026.

[19] H. J. Fatih, M. Ashengroph, and A. Sharifi, "Potent Antibacterial , Anti-Biofilm and Anti- Virulence Agent Against Pathogenic Bacteria," *BMC Microbiol.*, vol. 24, no. 535, pp. 1–13, 2024.

[20] M. A. Mohaisen and M. M. Sirhan, "Study of Fe3O4-NPs Coated with an Alcoholic Extract of C. Spinosa to Identify Appropriate IC50 HTC116 Cancer Cells," *Pakistan J. Anal. Environ. Chem.*, vol. 25, no. 1, pp. 99–112, 2024, doi: 10.21743/PJAEC/2024.06.10.

[21] A. A. M. Saeed, E. M. A. Mohsen, and A. R. A. Bin Yahia, "Eco-friendly synthesis, characterization, and anticancer potential of iron oxide nanoparticles derived from Plectranthus amboinicus and Dorstenia foetida plant extracts," *Green Chem. Lett. Rev.*, vol. 18, no. 1, 2025, doi: 10.1080/17518253.2025.2525090.

[22] N. A. Zakariya, W. H. W. Jusof, and S. Majeed, "Green Approach for Iron Oxide Nanoparticles Synthesis: Application in Antimicrobial and Anticancer- an Updated Review," *Karbala Int. J. Mod. Sci.*, vol. 8, no. 3, pp. 421–437, 2022, doi: 10.33640/2405-609X.3256.

[23] B. A. Shah *et al.*, " Synergistic Antibacterial Activity of Fe 3 O 4 @mPEG-Ag Nanoparticles with Molecular Docking Analyses ," *BME Front.*, vol. 6, pp. 1–21, 2025, doi: 10.34133/bmef.0214.

[24] S. Azadi *et al.*, "Fe 3 O 4 @ SiO 2 / Schiff-base / Zn (II) nanocomposite functioning as a versatile antimicrobial agent against bacterial and fungal pathogens," no. Ii, pp. 1–16, 2025.

[25] A. Taufiq *et al.*, "Synthesis of Fe3O4/Ag nanohybrid ferrofluids and their applications as antimicrobial and antifibrotic agents," *Heliyon*, vol. 6, no. 12, 2020, doi: 10.1016/j.heliyon.2020.e05813.

[26] S. Dabagh, S. A. Haris, B. K. Isfahani, and Y. N. Ertas, "Silver-Decorated and Silica-Capped Magnetite Nanoparticles with Effective Antibacterial Activity and Reusability," *ACS Appl. Bio Mater.*, vol. 6, no. 6, pp. 2266–2276, 2023, doi: 10.1021/acsabm.3c00122.

[27] C. Serrano *et al.*, "Chemical Profile and Biological Activities of Brassica rapa and Brassica napus Ex Situ Collection from Portugal," *Foods*, vol. 13, no. 8, 2024, doi: 10.3390/foods13081164.

[28] A. A. Jabbar, C. H. Saeed, S. M. Abdulaziz, and B. J. Mahmood, "Chemical Differentiation and Antimicrobial Potential of Four Brassica napus L Seed Oils," *Iraqi J. Sci.*, vol. 62, no. 12, pp. 4597–4613, 2021, doi: 10.24996/ijs.2021.62.12.1.

[29] A. ABAZA, "Isolation and Identification of Defensive Flavonoids From Brassica Napus Leaves Extract With Promising Biological Activity To Control the Cotton Leafworm, Spodoptera Littoralis (Boisd.)," *Egypt. J. Agric. Res.*, vol. 96, no. 1, pp. 47–64, 2018, doi: 10.21608/ejar.2018.129663.

[30] P. Properties, "Brassica Genus Seeds : A Review on Phytochemical Screening," pp. 1–34, 2022.

[31] S. Iravani, "Green synthesis of metal nanoparticles using plants," *Green Chem.*, vol. 13, no. 10, pp. 2638–2650, 2011, doi: 10.1039/c1gc15386b.

[32] S. Bano, M. Agrawal, and D. Pal, "A review on green synthesis of silver

nanoparticle through plant extract and its medicinal Applications," *J. Indian Chem. Soc.*, vol. 97, no. 7, pp. 983–988, 2020.

[33] S. Saedi, M. Shokri, and J. W. Rhim, "Antimicrobial activity of sulfur nanoparticles: Effect of preparation methods," *Arab. J. Chem.*, vol. 13, no. 8, pp. 6580–6588, 2020, doi: 10.1016/j.arabjc.2020.06.014.

[34] M. A. Mohaisen and M. M. Sirhan, "Synthesis and Characterization of Fe 3 O 4 -NPs from Leaves C . Spinosa Extracts and their Anti-Microbial Activity," vol. 3, no. 3, pp. 69–89, 2024.

[35] K. Okaiyeto, M. O. Ojemaye, H. Hoppe, L. V Mabinya, and A. I. Okoh, "Phytofabrication of Silver / Silver Chloride Oedera genistifolia : Characterization and Antibacterial Potential".

[36] A. Mustafa, U. Ali, A. Iqbal, M. Qayyum, I. U. Haq, and F. Islam, "Synthesis and Characterization of Fe 3 O 4 Nanoparticles by Sol-Gel Method Using Water as a Solvent," vol. 14, no. 1, pp. 1–11, 2025, doi: 10.4236/anp.2025.141001.

[37] C. Garai, "Rasayan Green synthesis , characterization and applications of metal nanoparticles

_____

____ Prayogik Rasayan," vol. 2, no. 3, pp. 42–45, 2018, doi: 10.53023/p.rasayan-20180718.

[38] S. H. Alwasel, "DPPH Radical Scavenging Assay ˙," 2023.

[39] S. Razmavar, M. A. Abdulla, S. B. Ismail, and P. Hassandarvish, "Antibacterial activity of leaf extracts of Baeckea frutescens against methicillin-resistant Staphylococcus aureus," *Biomed Res. Int.*, vol. 2014, 2014, doi: 10.1155/2014/521287.

[40] E. A. Tendencia, "Chapter 2. Disk diffusion method.," *Lab. Man. Stand. methods Antimicrob. Sensit. tests Bact. Isol. from Aquat. Anim. Environ.*, pp. 13–29, 2004.

[41] S. Bassim, "Green Synthesis of Fe3O4 Nanoparticles and its Applications in Wastewater Treatment .," pp. 1–36, 2022.

[42] T. T. Win, S. Khan, B. Bo, S. Zada, and P. Fu, "Green synthesis and characterization of - nanoparticles using Chlorella ‑ K01 extract for potential enhancement of plant growth stimulating and antifungal activity," pp. 1–11, 2021, doi: 10.1038/s41598-021-01538-2.

[43] M. Yoga, N. Imani, and N. Adrianto, "Results in Chemistry Green synthesis of Fe 3 O 4 / Ag composite nanoparticles using Moringa oleifera : Exploring microstructure , optical , and magnetic properties for magnetic hyperthermia applications," *Results Chem.*, vol. 6, no. March, p. 100999, 2023, doi: 10.1016/j.rechem.2023.100999.

[44] B. A. Eldeeb, W. M. Abd, E. Raheem, and S. Elbeltagi, "Green synthesis of biocompatible Fe 3 O 4 magnetic nanoparticles using Citrus Sinensis peels extract for their biological activities and magnetic ‑ hyperthermia applications," *Sci. Rep.*, no. 0123456789, pp. 1–12, 2023, doi: 10.1038/s41598-023-46287-6.

[45] A. You, M. Be, and I. In, "Synthesis and Characterization of Nanoparticle Magnetite," vol. 020137, no. May 2017, pp. 4–9, 2019.

[46] M. R. Ghazanfari, M. Kashefi, S. F. Shams, and M. R. Jaafari, "Perspective of Fe 3 O 4 Nanoparticles Role in Biomedical Applications," vol. 2016, 2016, doi: 10.1155/2016/7840161.

[47] A. F. Jalal and N. A. Fakhre, "Preparation and Characterization of Green Fe 3 O 4 Nanoparticle Using the Aqueous Plant Extract of Gundelia tournefortii L .," pp. 58–63,

ISSN 2072-3857

2020, doi: 10.14500/aro.10843.

[48] R. F. Ajayi, S. Tshoko, C. Franke, N. Ngema, V. Thipe, and T. Mulaudzi, "Mixtures for the Synthesis of Graphene Silver and Zinc Oxide Nanocomposites," pp. 61–81, 2022, doi: 10.4236/jsemat.2022.124005.

[49] I. L. Botto, S. Tuti, M. J. Gonzalez, D. Gazzoli, D. Scienze, and U. R. Tre, "Correlation between Iron Reducibility in Natural and Iron-Modified Clays and Its Adsorptive Capability for Arsenic Removal," no. May, pp. 129–139, 2016.

[50] L. P. Yan, S. C. B. Gopinath, S. Subramaniam, Y. Chen, P. Velusamy, and S. V Chinni, "Greener synthesis of nanostructured iron oxide for medical and sustainable agro-environmental bene fi ts," no. September, pp. 1–15, 2022, doi: 10.3389/fchem.2022.984218.

[51] F. Chen, N. Ilyas, X. Liu, Z. Li, S. Yan, and H. Fu, "Size Effect of Fe 3 O 4 Nanoparticles on Magnetism and Dispersion Stability of Magnetic Nano fl uid," vol. 9, no. November, pp. 1–9, 2021, doi: 10.3389/fenrg.2021.780008.

[52] F. V Gutierrez *et al.*, "Magnetic Characterization by Scanning Microscopy of Functionalized Iron Oxide Nanoparticles," pp. 1–19, 2021.

[53] E. R. Carmona *et al.*, "Sustainable Green Synthesis of Fe 3 O 4 Nanocatalysts for Efficient Oxygen Evolution Reaction," pp. 1–13, 2025.

[54] Y. P. Yew, K. Shameli, M. Miyake, N. Kuwano, N. Bahiyah, and B. Ahmad, "Green Synthesis of Magnetite (Fe 3 O 4) Nanoparticles Using Seaweed (Kappaphycus alvarezii) Extract," *Nanoscale Res. Lett.*, 2016, doi: 10.1186/s11671-016-1498-2.

[55] R. Khatun *et al.*, "Phytochemical-Assisted Synthesis of Fe 3 O 4 Nanoparticles and Evaluation of Their Catalytic Activity," pp. 1–10, 2022.

[56] M. Eslamdoust and F. Samari, "One-pot green synthesis of Fe 3 O 4 @ ZnO core – shell nanocomposites with multifunctional properties," pp. 1–18, 2025.

[57] A. Mohapatra and I. Park, "Recent Advances in ROS-Scavenging Metallic Nanozymes for Anti-Inflammatory Diseases : A Review," pp. 13–23, 2023.

[58] M. Nanoparticles, "The Antioxidant Effect of the Metal and," 2022.

[59] B. Patel *et al.*, "RSC Advances Green synthesis of Ag – Fe bimetallic nanoparticles using fungal fi ltrates : unlocking multifunctional medical and environmental applications †," *RSC Adv.*, vol. 15, pp. 1565–1575, 2025, doi: 10.1039/D4RA07541B.

[60] S. H. Alrefaee, "Plasma creator device to produce Fe @ C core – shell : anti ‐ bacterial , anti ‐ oxidant , anti ‐ diabetic , anti ‐ inflammatory , and cytotoxic activities," *J. Saudi Chem. Soc.*, vol. 29, no. 4, pp. 1–12, 2025, doi: 10.1007/s44442-025-00017-x.

[61] N. E. Al and H. Deyala, "Antioxidant and Antibacterial Activities of Nano ‐ probiotics Versus Free Probiotics Against Gastrointestinal Pathogenic Bacteria," *Indian J. Microbiol.*, vol. 64, no. 1, pp. 141–152, 2024, doi: 10.1007/s12088-023-01140-2.

[62] M. Kumar, S. Puri, A. Pundir, S. P. Bangar, and S. Changan, "Composition of Selected Medicinal Plants for Therapeutic Uses from Cold Desert of Western Himalaya," 2021.

[63] A. L. P. Cruz, J. A. G. Cervantes, X. G. V. Anzaldo, and G. G. Rivas, "Synthesis and design of Ag – Fe bimetallic nanoparticles as antimicrobial synergistic combination

therapies against clinically relevant pathogens," *Sci. Rep.*, pp. 1–10, 2021, doi: 10.1038/s41598-021-84768-8.

[64] I. Santos, A. Sousa, A. Vale, F. Carvalho, E. Fernandes, and M. Freitas, "Protective effects of flavonoids against silver nanoparticles ‐ induced toxicity," *Arch. Toxicol.*, no. 0123456789, 2025, doi: 10.1007/s00204-025-04068-2.

[65] I. Rahayu, E. Prihatini, R. Ismail, W. Darmawan, and L. Karlinasari, "Fast-Growing Magnetic Wood Synthesis by an In-Situ Method," 2022.

[66] S. Sharma *et al.*, "Green synthesis and characterization of Ag- Fe bivalent nanoparticles for One Health management and environmental sustainability," *Eur. J. Mater.*, vol. 5, no. 1, p., 2025, doi: 10.1080/26889277.2025.2560336.

[67] F. Mwangi, "Green Synthesis of Metal Oxide Nanoparticles Using Plant Extracts : Applications in Catalysis and Biomedicine," 2026.

[68] U. O. Aigbe and O. A. Osibote, "Journal of Hazardous Materials Advances Green synthesis of metal oxide nanoparticles , and their various applications," *J. Hazard. Mater. Adv.*, vol. 13, no. September 2023, p. 100401, 2024, doi: 10.1016/j.hazadv.2024.100401.

ISSN 2072-3857